Annals of Botany **122**: 251–265, 2018
doi: 10.1093/aob/mcy058, available online at www.academic.oup.com/aob

ANNALS OF BOTANY
Founded 1887

miR172 downregulates the translation of *cleistogamy 1* in barley

Nadia Anwar[1], Masaru Ohta[1,2], Takayuki Yazawa[1], Yutaka Sato[1,2], Chao Li[1], Akemi Tagiri[1], Mari Sakuma[1], Thomas Nussbaumer[3,4], Phil Bregitzer[5], Mohammad Pourkheirandish[1,2,6], Jianzhong Wu[1,2] and Takao Komatsuda[1,2,*]

[1]National Institute of Agrobiological Sciences, Tsukuba, 305 8602 Japan, [2]National Agriculture and Food Research Organization (NARO), Tsukuba, 305 8602 Japan, [3]Munich Information Center for Protein Sequences, Institute of Bioinformatics and Systems Biology, Helmholtz Center Munich, 85764 Neuherberg, Germany, [4]Division of Computational System Biology, Department of Microbiology and Ecosystem Science, University of Vienna, 1090 Vienna, Austria, [5]USDA-ARS, National Small Grains Germplasm Research Facility, Aberdeen, ID 83210, USA and [6]The University of Sydney, Faculty of Agriculture and Environment, Plant Breeding Institute, Cobbitty, NSW 2570, Australia
**For correspondence. E-mail takao@affrc.go.jp*

Received: 8 November 2017 Returned for revision: 16 January 2018 Editorial decision: 21 March 2018 Accepted: 30 April 2018
Published electronically 22 May 2018

• **Background and Aims** Floret opening in barley is induced by the swelling of the lodicule, a trait under the control of the *cleistogamy1* (*cly1*) gene. The product of *cly1* is a member of the APETALA2 (AP2) transcription factor family, which inhibits lodicule development. A sequence polymorphism at the miR172 target site within *cly1* has been associated with variation in lodicule development and hence with the cleistogamous phenotype. It was unclear whether miR172 actually functions in *cly1* regulation and, if it does, which miR172 gene contributes to cleistogamy. It was also interesting to explore whether miR172-mediated *cly1* regulation occurs at transcriptional level or at translational level.
• **Methods** Deep sequencing of small RNA identified the miR172 sequences expressed in barley immature spikes. miR172 genes were confirmed by computational and expression analysis. miR172 and *cly1* expression profiles were determined by *in situ* hybridization and quantitative expression analysis. Immunoblot analysis provided the CLY1 protein quantifications. Definitive evidence of the role of miR172 in cleistogamy was provided by a transposon *Ds*-induced mutant of *Hv-miR172a*.
• **Key Results** A small RNA analysis of the immature barley spike revealed three isomers, miR172a, b and c, of which miR172a was the most abundant. *In situ* hybridization analysis showed that miR172 and *cly1* co-localize in the lodicule primordium, suggesting that these two molecules potentially interact with one another. Immunoblot analysis showed that the sequence polymorphism at the miR172 target site within *cly1* reduced the abundance of the CLY1 protein, but not that of its transcript. In a *Ds*-induced mutant of *Hv-miR172a*, which generates no mature miR172a, the lodicules fail to grow, resulting in a very small lodicule.
• **Conclusions** Direct evidence is presented to show that miR172a acts to reduce the abundance of the CLY1 protein, which enables open flowering in barley.

Key words: MicroRNA, lodicule, *AP2*, translation, cereals.

INTRODUCTION

The floral morphology of the grasses differs significantly from that of other angiosperms (Ciaffi *et al.*, 2011). The grass homologue of the dicotyledonous inner perianth whorl (which is the petal for most dicots) is the lodicule, a pair of which lies at the base of the grass pistil and stamen (Bommert *et al.*, 2005). In a non-cleistogamous [wild-type (WT)] floret, the lodicules swell just prior to anthesis, pushing apart the palea and lemma, thereby releasing pollen and exposing the stigma to non-self pollen (Fig. 1A, left panel). In the cleistogamous floret (Fig. 1A, right panel), by contrast, this swelling does not occur, with the result that pollen is released within a closed floret, thereby forcing self-fertilization (Briggs, 1978; Lord, 1981). In the ecology and evolution of plants, it has been proposed that adaptive plasticity of cleistogamy could be driven by variation in the pollination environment, with cleistogamous flowers providing reproductive assurance when pollinators are scarce and non-cleistogamous flowers reducing inbreeding depression in offspring when pollinators are abundant (Stojanova *et al.*, 2016). Cleistogamous barley cultivars are better able to avoid infection by *Fusarium* species that cause fusarium head blight, by denying entry to spores during early stages of floret and kernel development and showing coincident quantitative trait loci for blight resistance and *cly1* (Yoshida *et al.*, 2005; Hori *et al.*, 2006; Sato *et al.*, 2008), and they also greatly reduce the risk of gene flow through pollen dispersal (Daniell, 2002; Abdel-Ghani *et al.*, 2004; Ma and Wang, 2004). On the other hand, non-cleistogamy is essential for the production of F_1 hybrid grain.

The analysis of natural variants in barley demonstrated that cleistogamy is determined by the single recessive gene *cleistogamy1* (*cly1*) (Turuspekov *et al.*, 2004; Honda *et al.*, 2005). The product of this gene (CLY1) is an APETALA2 (AP2)-type

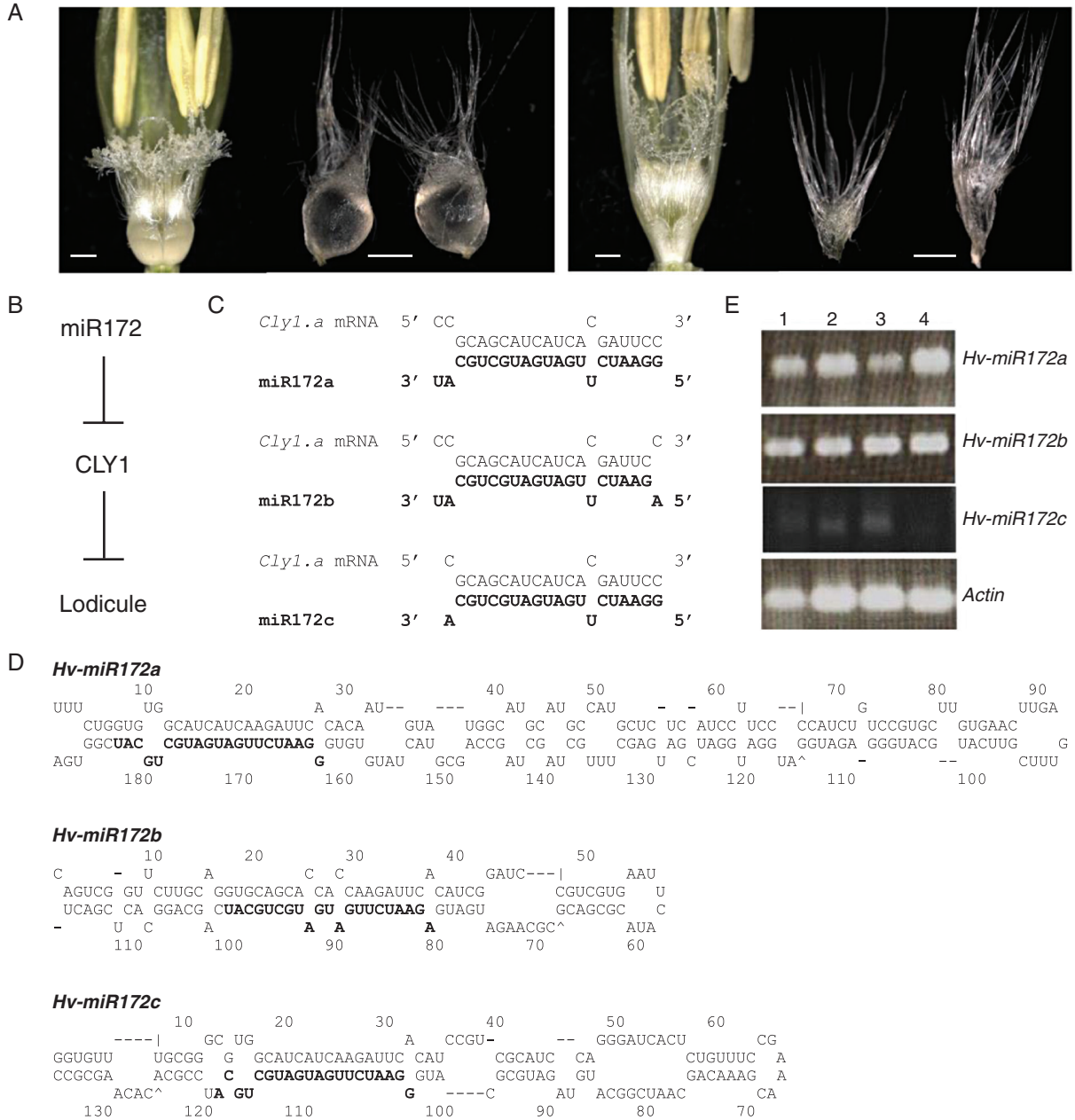

FIG. 1. The barley inflorescence and the *Hv-miR172* genes. (A) Variation in lodicule size at anthesis. (Left) AZ (non-cleistogamous). (Right) KNG (cleistogamous). Scale bar = 0.5 mm. (B) Scheme of proposed interaction between miR172 and CLY1 for lodicule development. The *Cly1.a* and *cly1.b* alleles both encode CLY1, which suppresses the development of lodicules. Expression of *Cly1.a* is negatively regulated by miR172, resulting in less suppression of lodicule development by CLY1. (C) Potential interactions between *cly1* mRNA and miR172 isoforms in cultivar 'Morex'. Bold letters indicate miR172 sequences that can potentially bind with *cly1* mRNA sequence. (D) *In silico* predicted hairpin secondary structure of the miR172 precursors. Bold text indicates the mature miRNA sequence. Precursor sequence length and free folding energy (ΔG) for *Hv-miR172a*, *b* and *c* were, respectively, 189 nt and −92.80 kcal mol^{-1}, 117 nt and −58.20 kcal mol^{-1} and 135 nt and −63.60 kcal mol^{-1}. (E) RT–PCR-derived abundance of primary miR172s in the immature spikes at the awn primordium stage. Lane 1, AZ; lane 2, KNG; lane 3, 'Morex'; lane 4, 'Golden Promise'. *Actin* was the chosen reference sequence.

transcription factor (Nair *et al.*, 2010). A single synonymous nucleotide polymorphism within the *cly1* coding sequence differentiates the *cly1.b* (cleistogamous) from the *Cly1.a* (non-cleistogamous) sequence. This polymorphic site lies within a 21-nucleotide (nt) sequence targeted by the micro-RNA (miRNA) miR172 (Supplementary Data Fig. S1A), and is thought to disrupt the interaction between miR172 and *cly1* transcript (Nair *et al.*, 2010). In non-cleistogamous barleys, the assumption is that miR172 downregulates *cly1*, resulting in the development of normal lodicules. Besides the proposed miR172-directed post-transcriptional regulation (Fig. 1B), *cly1* has been shown to be regulated at transcriptional level by an epiallele that represses *cly1* transcription independently of miR172 action (Wang *et al.*, 2015).

The miRNAs perform a variety of regulatory functions in plant development (Bartel, 2004). Their mature form is

represented by short (21–24 nt) sequences able to either induce the degradation of a target mRNA or to inhibit its translation. Their specificity relies on sequence complementarity with the target. The target of miR172 is the transcript of the *AP2* gene (Park *et al.*, 2002; Chen, 2004), along with a small group of *AP2*-like genes (Aukerman and Sakai, 2003; Schmid *et al.*, 2003; Schwab *et al.*, 2005). The gene encoding miR172 is transcribed by RNA polymerase II and a full-length miRNA transcript termed 'primary miR172' (pri-miR172) is then processed to form a 21-bp RNA duplex consisting of the active strand and its complementary strand (Xie *et al.*, 2005; Mateos *et al.*, 2010). The various miR172s function in floral development, including floral transition and floral patterning (Lauter *et al.*, 2005; Chuck *et al.*, 2007; Zhu *et al.*, 2009; Luo *et al.*, 2013; Yumul *et al.*, 2013), roles that have been retained throughout the angiosperms. The present study sought to identify the set of barley miR172 genes, and to determine which (if any) contribute to cleistogamy. A secondary aim was to explore whether the downregulation of *cly1* by miR172 operates through either the cleavage of *cly1* mRNA, as previously anticipated (Nair *et al.*, 2010), or the inhibition of *cly1* translation.

MATERIALS AND METHODS

Plant materials

The barley cultivar 'Azumamugi' (AZ, NIAS GenBank accession number JP17209) was taken as representative of the non-cleistogamous type, while cultivar 'Kanto Nakate Gold' (KNG, JP15436) was used as the cleistogamous type. The material was sown in the field during the autumn at Tsukuba, with an inter-plant and inter-row spacing of 20 and 80 cm, respectively. The *Ds*-induced mutant *Ds-miR172a*, which harbours a *Ds* element inserted into one of the barley miR172 in a cultivar 'Golden Promise' (USDA-ARS accession number PI 343079) background (Brown and Bregitzer, 2011) was crossed and backcrossed with the non-cleistogamous cultivar 'Conlon' (PI 597789), and the resulting BC_1F_2 progeny were raised in a greenhouse.

Measurement of lodicule volume

At least three randomly selected spikes, including the flag leaf and peduncle, were taken from each entry at the yellow anther stage (Kirby and Appleyard, 1981) and florets were sampled from the central portion of the spikes. After removing the lemma, the lodicules were photographed and the resulting images were used to measure lodicule width and depth (surrogates of lodicule volume), following Nair *et al.* (2010).

Sequencing and bioinformatic analysis of small RNAs (sRNAs)

An sRNA library prepared from immature spikes of the barley cultivar 'Morex' (Wang *et al.*, 2015) was sequenced, and reads in the length range 17–36 nt were sorted into unique sequences, retaining a count of copy number to generate the metric 'number of reads per million reads' (RPM). MOODS software (Korhonen *et al.*, 2009) was employed as an aligner to identify any set of miRNAs potentially targeting *cly1*, by allowing a maximum of six mismatches between the miRNA sequence and the *cly1* full-length cDNA (flcDNA) including untranslated region (UTR) sequence. The sequences were then filtered based on a penalty score whereby each mismatch was assigned a score of 1, a wobble (G:U) mismatch a score of 0.5 and a bulge in either RNA strand a score of 2. The threshold score for retention of a candidate was 4.0, following the selection criterion of 3.5 as described by Jones-Rhoades and Bartel (2004). The approach based on a penalty score is used frequently (Lelandais-Briere *et al.*, 2009; Joshi *et al.*, 2010; Kim *et al.*, 2012). The selected sequences were then subjected to a search against the miRBase (http://microrna.sanger.ac.uk) set of all known miRNAs (Kozomara *et al.*, 2011) using the BLAST+ algorithm (Camacho *et al.*, 2009), and assigned to their best-match miRNA family. To identify miRNAs that could potentially bind to an miR172 target site, we also used the BLAST+ 'blast-short' and psRNATarget (Dai and Zhao, 2011) as the aligner and the target prediction program, respectively.

Identification of barley miR172 genes

The selected miRNA sequences were aligned against the 'Morex' whole-genome sequence (WGS) (Mayer *et al.*, 2012) through the use of Bowtie software (Langmead *et al.*, 2009). Sequences that aligned perfectly were considered to be a putative coding locus for a given miRNA. The 400-nt context of an miR172 site was used to predict the energetically most favourable RNA secondary structure, based on the RNA folding prediction program mfold v3.5 (Zuker, 2003). These structures were evaluated based on three criteria: (1) the ability to fold into a stem–loop structure with the mature miRNA located on the stem–loop's helical region; (2) a maximal free folding energy (mfe) lower than that of tRNA and rRNA; and (3) a predicted mature miRNA: its complementary miRNA duplex having fewer than six mismatches and a maximum of three nucleotides present in any loop or bulge (Zhang *et al.*, 2006; Qiu *et al.*, 2007; Xie *et al.*, 2007). GENETYX v8.0 software (Software Development, Tokyo, Japan) was used to perform a multiple sequence alignment of barley miR172 precursor sequences with those represented in miRBase.

DNA extraction, PCR amplification and sequencing

Genomic DNA was extracted from leaves and immature spikes following Komatsuda *et al.* (1998). The primers used to amplify and sequence the amplicons are detailed in Supplementary Data Table S1. Each 10-μL PCR contained 25 ng of template, 0.5 U of ExTaq DNA polymerase (Takara, Tokyo, Japan), 1× buffer, 2.5 mM $MgCl_2$, 200 μM dNTP and 300 nM of each primer, and the cycling regime comprised a 94 °C/5 min denaturation, followed by 30 cycles of 94 °C/30 s, 55–60 °C (primer-dependent)/30 s, 72 °C/60 s, with a final 72 °C/10 min extension. The amplicons were purified using a QIAquick PCR Purification kit (Qiagen, Tokyo, Japan) before submission for sequencing. The *Ds-miR172a* mutant was PCR-validated by amplifying from a *Ds*-specific primer (Ds3325F)

in conjunction with an miR172a-specific primer (508-3′ R) (Brown and Bregitzer, 2011). The allelic state at *Cly1* was determined by a genotypic test based on the marker P101AP25′ *Nmu*CI (Nair *et al.*, 2010).

RNA extraction, reverse transcription PCR (RT–PCR) and quantitative real time PCR (qRT–PCR)

Total RNA was extracted using a mirVana miRNA Isolation Kit (Life Technologies) from a bulk sample of three to ten immature spikes that had been developmentally staged (Kirby and Appleyard, 1981). The RNA was quantified using a NanoDrop 1000 device (Thermo Fisher Scientific, Waltham, MA, USA), then treated with RNase-free DNase (Takara Bio, Otsu, Japan) to remove any contaminating genomic DNA. The cDNA first strand was synthesized using the SuperScript III system (Invitrogen, Carlsbad, CA, USA) primed by oligo-dT, to provide the template for RT–PCRs based on primers listed in Supplementary Data Table S1. A series of 25-µL qRT–PCRs was based on the TaqMan system (probe and primer details given in Supplementary Data Table S1). The barley *Actin* gene (accession number DN182500) was used as the reference. In a study conducted to identify a suitable reference gene across diverse barley cultivars and tissues, *Actin* was identified as the only traditional reference gene that demonstrated a highly reliable and stable expression pattern (Gines *et al.*, 2017). All reactions were performed on a CFX96 Real-Time System device (Bio-Rad, Tokyo). The abundance of each pri-miR172 transcript was quantified in a 25-µL qRT–PCR containing 900 nM forward and reverse primers for 3′ end unique sequence of pri-miR172 (except for miR172b, for which 600 nM of each primer was used), 200 nM fluorescein amidite (FAM) double-quenched TaqMan miR172 probe, 120 nM primers targeting *Actin*, 120 nM Texas Red double-quenched TaqMan *Actin* probe and 2× SsoAdvanced Universal Probe Supermix (Bio-Rad, Tokyo, Japan). The cycling parameters were 95 °C/30 s, followed by 50 cycles of 95 °C/10 s, 57 °C/15 s. The abundance of *cly1* transcript was quantified using 900 nM of each primer and 250 nM of the TaqMan *cly1* probe (Supplementary Data Table S1) in TaqMan Gene Expression Master Mix (Applied Biosystems, Life Technologies Japan, Tokyo). The cycling regime consisted of a 95 °C/10 min denaturation, followed by 40 cycles of 92 °C/30 s, 60 °C/60 s and a final 60 °C/10 min extension. *Actin* was quantified using 300 nM of each primer and 200 nM *Actin* TaqMan probe in 2× SsoAdvanced Universal Probe Supermix, with a cycling regime of 95 °C/30 s, followed by 45 cycles of 95 °C/10 s, 57 °C/15 s. The transcript abundance of the barley *Q* gene homologue was quantified using 600 nM of each primer and 200 nM of the relevant TaqMan probe (Supplementary Data Table S1) in 2× SsoAdvanced Universal Probe Supermix, with a cycling regime of 95 °C/30 s, followed by 45 cycles of 95 °C/10 s, 52 °C (*Q* exon 10) or 64 °C (*Q* 3′-UTR)/30 s. *Actin* was quantified in a separate reaction as described above. At least three biological replicates per sample were run, with each replicate represented by at least three technical replicates. To determine the absolute abundance of individual transcripts, the relevant fragment was cloned into pCR4-TOPO (Invitrogen, Carlsbad, CA, USA) and a serial dilution of recombinant plasmids was used to generate a standard curve. The raw C_T values were converted into an absolute copy number by the use of a standard curve. Relative abundances of each transcript were calculated from (target mRNA copy number ng^{-1} total RNA)/(*Actin* mRNA copy number ng^{-1} total RNA).

Quantification of mature miR172

A qRT–PCR targeting mature miR172 was performed using the TaqMan MicroRNA assay (Applied Biosystems) (for details see Supplementary Data Table S1), following the manufacturer's protocol. The small nucleolar RNA (snoRNA) *Hv-snoR13* was used as an endogenous control (http://bioinf.scri.sari.ac.uk/cgi-bin/plant_snorna/home), because it is both abundant and stable, because its size is close to that of miRNAs, because its assay format is similar to that of miRNAs, and because it is unlikely to be involved in any miRNA regulatory pathway. The qRT–PCR was achieved via a customized TaqMan small RNA assay (Applied Biosystems, Tokyo, Japan), which comprised a specific stem–loop reverse transcription primer along with appropriate conventional primers and an FAM dye-labelled probe (Supplementary Data Table S1). Quantification of mature miR172s was based on the $^{\Delta\Delta C}{}_T$ method (Livak and Schmittgen, 2001), and the data are presented in the form of fold differences following normalization against the abundance of *snoR13* present at the stamen primordium stage. At least three biological replicates at each developmental stage were performed, and each replicate was represented by at least three technical replicates.

RNA in situ *hybridization*

Immature spikes were fixed, processed and sectioned as described by Komatsuda *et al.* (2007). Double digoxigenin (DIG)-labelled miRCURY Locked Nucleic Acid (LNA) miRNA detection probes (Supplementary Data Table S1) complementary to miR172a, miR172b and a scrambled miRNA (control) were purchased from Exiqon (Foster City, CA, USA) for the detection of mature miR172s. Each slide was treated with 180 µL of hybridization solution containing 0.225 µL of 25 µM probe, and the subsequent hybridization and washing steps were performed at either 55 °C (miR172) or 60 °C (*snoR13*). To detect *cly1* mRNA, the probe used was a 280-nt fragment amplified from the *cly1* 3′-UTR (primers are given in Supplementary Data Table S1), while for the *Q* orthologue the probe was a 265-nt fragment amplified from the 3′-UTR (primers are given in Supplementary Data Table S1). For *cly1* and *Q* hybridization, each slide was treated with 180 µL of hybridization solution containing 0.1–0.25 µL of probe generated by a DIG RNA labelling mix according to the manufacture's protocol (Roche, Mannheim). The subsequent *in vitro* transcription and *in situ* hybridization protocols followed methods described by Komatsuda *et al.* (2007).

Laser microdissection

Immature spikes were fixed by vacuum infiltration in cold 75 % ethanol/25 % acetate, and embedded in paraffin using a microwave

processor (Energy Beam Sciences, East Granby, CT, USA) following Takahashi *et al.* (2010). The paraffin-embedded samples were cut into 10-µm thick sections using an RM2255 microtome (Leica Microsystems, Wetzlar, Germany), which were then subjected to laser microdissection using a Veritas Laser Microdissection System LCC1704 device (Life Technologies). Total RNA was extracted from the samples using a Pico-Pure RNA Isolation Kit (Life Technologies), following the manufacturer's protocol. The quantity and quality of the RNA obtained were checked with a 2100 Bioanalyzer (Agilent Technologies, Santa Clara, CA, USA). The synthesis of cDNA and subsequent qRT–PCRs were performed as described above.

Immunoblotting analysis

A synthetic NH_2-LQKNGFHSLARPT-OH peptide (CLY1 positions 475–487) was inoculated into rabbits to derive a polyclonal antibody (Sigma-Aldrich, St Louis, MO, USA). The antiserum was passed through an affinity column containing the epitope peptide. A monoclonal antibody against α-tubulin was purchased from Sigma-Aldrich (St Louis, MO, USA). Immature barley spikes were frozen in liquid nitrogen and stored at −80 °C until required. A bulk of five to ten spikes was first coarsely crushed, then finely homogenized in a BioMasher II device (Nippi, Tokyo, Japan). The resulting powder was extracted in 100 µL of 50 mM Tris–HCl (pH7.5)/150 mM NaCl/0.5 % v/v Triton X100/5 mM EDTA/5 mM EGTA and 1× complete EDTA-free Mini Protease Inhibitor mixture (Roche, Basel, Switzerland) and centrifuged (3000 *g*, 10 min), and the supernatant was denatured by adding 100 µL of 50 mM Tris–HCl (pH 6.8)/2 % w/v SDS/6 % v/v 2-mercaptoethanol/bromophenol blue (BPB)/10 % v/v glycerol, and holding at 65 °C for 10 min. The proteins were electrophoretically separated using a 10 % polyacrylamide gel, then electrophoretically transferred to a PVDF membrane (Merck Millipore, Darmstadt, Germany). The membranes were initially challenged with a 1/5000 dilution of primary antibody in 10 mM Tris–HCl (pH7.5)/150 mM NaCl/0.1 % v/v Tween 20/1 % w/v skimmed milk, rinsed thoroughly, then incubated in a 1/10 000 dilution of horseradish peroxidase-conjugated anti-rabbit immunoglobulin G (IgG) (for CLY1) or a 1/10 000 dilution of anti-mouse IgG (for α-tubulin) in the same buffer. Signal was detected using ImmunoStar (Wako, Osaka, Japan) and ImageQuant LAS3000 (GE Healthcare, Chalfont St Giles, UK), and its intensity was analysed using Multi Gauge v2.0 software (Fujifilm, Tokyo, Japan).

RESULTS

Mature miR172s detected in sRNA library

A total of 150 million sRNA reads (accession number DRA006260) were recovered from the 'Morex' immature spike library by Wang *et al.* (2015). After removal of adaptor sequences, rRNAs and tRNAs, and filtering by length (17–36 nt), a set of 124 196 599 (mean length 25.1 nt) was retained. These resolved into 22 755 479 unique sequences (mean length 24.4 nt) to form the population of putative sRNAs (Supplementary Data Fig. S1B). The length, distribution and abundance of sRNA reads is shown in Supplementary Data Figure S1B, where the analysis range was expanded in order to capture the existence of unusual types of miRNAs as referred by Kim *et al.* (2012). When the sRNAs were aligned with the 'Morex' *cly1* flcDNA sequence, the most hits (Supplementary Data Fig. S1A) were obtained in the region between positions 1850 and 1870 conserved in plants (Supplementary Data Fig. S1C). Applying the filter within the MOODS software based on a maximum penalty score of 4.0 and RPM >1 to the miRNAs complementary to the target site (Table 1) identified three distinct sequences: miR172a (21 nt), b (21 nt) and c (20 nt) (Fig. 1C). miR172a differed from b at the 5′ end (G versus A), while c lacked the 3′ terminal U (Table 1). The sequence of miR172a is identical to the miR172 species that was interrupted by a *Ds* insertion (Brown and Bregitzer, 2011). The three barley miR172s were conserved in plants (Supplementary Data Fig. S1C) and the hybrids between each of the isoforms and *cly1* mRNA (Fig. 1C) passed the complementarity criteria described by Jones-Rhoades and Bartel (2004). Thus, at least three mature miR172s produced in the immature barley spike appeared capable of interacting with *cly1* mRNA. Use of the blast-short and psRNATarget software packages produced an identical outcome (data not shown). The RPM counts for the three isoforms were, respectively, 70.9, 21.6 and 1.3 (Table 1), suggesting a difference of almost two orders of magnitude in their abundance.

Table 1. *Mature miR172s and corresponding genes in barley*

sRNA sequence (5′–3′)	Length	No. of reads	RPM[a]	Target site in *cly1*[b]	Penalty[c]	Mature miR172 identity[d]	Gene[d]	WGS contig ID[e]	Chromosome[e]
GGAAUCUUGAUGAUGCUGCAU	21	6693	70.9	1850–1870	3	miR172a	*Hv-miR172a*	Contig_38787	3HL
AGAAUCUUGAUGAUGCUGCAU	21	2036	21.6	1850–1870	4	miR172b	*Hv-miR172b*	Contig_49738	6HL
GGAAUCUUGAUGAUGCUGCA	20	118	1.3	1851–1870	2	miR172c	*Hv-miR172c*	Contig_1561881	7HS

[a]Reads per million; 10^6 × number of reads/total number of reads.

[b]Position of the *cly1* full-length cDNA (accession number KJ363931.1) aligned with miR172.

[c]Penalty score of each miRNA for the *cly1* is shown, calculated as 0.5 points assigned to each G:U wobble, 1 point to each non-G:U mismatch and 2 points to each bulged nucleotide in either RNA strand.

[d]IDs given in the present study.

[e]Based on miR172 isoform alignment to 'Morex' whole-genome sequencing contigs with no mismatches.

Identification of miR172 loci

When the miR172 isoform sequences were aligned with the 2 670 738 WGS contigs, perfect matches were obtained for miR172a on contig_38787 (chromosome arm 3HL), for miR172b on _49738 (chromosome arm 6HL) and for miR172c on _1561881 (chromosome arm 7HS) (Table 1). The location of miR172a on chromosome arm 3HL is consistent with the 3HL location as determined by wheat–barley chromosome addition lines (Brown and Bregitzer, 2011). To assess whether any of the genomic sequences was capable of forming the signature miR172 stem–loop hairpin, the selected region's secondary structure was analysed *in silico*. Each of the three sequences were predicted to fold into an appropriate stem–loop hairpin, and harboured the mature miR172 sequences on their 3′ arm. Thus, the encoding loci were denominated *Hv-miR172a*, *b* and *c* (Fig. 1D). Similarity between the precursors was limited to the sequences of the mature miRNA and its complementary (Supplementary Data Fig. S2). [Note that, similarly, the miR172 precursor sequences flanking the mature miRNA in other plant species are all highly divergent (Supplementary Data Fig. S2).] The miR172a locus is identical to GenBank accession HM243624, but neither miR172b nor miR172c has been identified previously. A subsequent RT–PCR experiment confirmed that all three genes were transcribed in the immature spike (Fig. 1E), although, in agreement with the RPM counts, the abundance of miR172c was very low (Table 1).

The abundance of pri-miR172 and mature product

The abundance of pri-miR172 was compared over the course of spike development in cultivars 'Azumamugi' (AZ, non-cleistogamous) and 'Kanto Nakate Gold' (KNG, cleistogamous). To distinguish between the pri-miR172s generated from the three genes, their divergent 3′-arm sequences (in close proximity to the stem–loop) was targeted (Supplementary Data Fig. S3A). A standard curve (Supplementary Data Fig. S4) was used to convert the raw C_T values into an absolute copy number. In AZ, the pri-miR172a RNA level was strongest during the lemma primordium stage, at which time it was considerably more abundant than in KNG (Fig. 2A). Its abundance was also higher in AZ than in KNG throughout the period between the glume primordium and stamen primordium stages. Mature miR172s determined by TaqMan miRNA assay were detected throughout the period of spike development (Fig. 2B), indicating that the miR172 sequences represented in the sRNA library were authentic. Their peak abundance occurred during the awn primordium stage, especially in AZ, in agreement with the abundance of pri-miR172s (Fig. 2A). This suggests that mature miR172s have a biological function, at least during the awn primordium stage, particularly in the non-cleistogamous cultivar AZ.

Abundance of cly1 *mRNA and CLY1 protein*

A qRT–PCR analysis was used to characterize the transcription behaviour of *cly1* over the period of spike development. When a pair of primers in the 3′-UTR was used (Supplementary Data Fig. S3B), the profiling showed that the gene was transcribed throughout the whole period (Fig. 2C), but that its transcript abundance was much higher (by almost 2-fold) when entering the awn primordium stage than earlier, consistent with the notion that CLY1 may regulate lodicule development. The temporal pattern of transcription was similar in AZ and KNG, and the transcript abundances were comparable (Fig. 2C). The abundance of the transcript remained comparable between the two cultivars (Fig. 2D) when a pair of primers flanking the miR172-binding site was used (Supplementary Data Fig. S3B). This result suggests that miR172-directed cleavage of *cly1* mRNA, if it occurs, is minor. It was thought that miR172 functions primarily via translational repression (Chen, 2004; Chuck *et al.*, 2007). This hypothesis was therefore tested by immunoblot analysis using an antibody raised against a C-terminal NH2-LQKNGFHSLARPT-OH peptide (positions 475–487) of CLY1. This sequence is unique to CLY1 and not found in other barley proteins by BLAST search. An immunoblot analysis showed that the level of CLY1 accumulated in KNG was ~3-fold higher ($P < 0.001$) than in AZ and their F_1 plants (Fig. 2E). Given that lodicules swell in the F_1 (Nair *et al.*, 2010), the lower levels of CLY1 in F_1 plants are consistent with this phenotype. Since the level of *cly1* transcript abundance was shown to be comparable in AZ and KNG (Fig. 2C, D), the clear inference was that miR172 compromises *cly1* translation efficiency. There was a difference of ~10-fold in of *cly1*/*Actin* transcript level ratio from the qPCR with the primer (Fig. 2C) and that with the exon 10 primers (Fig. 2D), but it is not unusual to see a lower signal with primers more distant from the 3′ end.

When the RNA template was extracted from spikelets and rachis separately using laser microdissection (Supplementary Data Fig. S5), once again the abundance of *cly1* mRNA in AZ proved to be similar to that in KNG, even when the primers used to amplify the template flanked the miR172 binding site (Fig. 3A). The abundance of miR172a transcript was similar in the spikelet and rachis, and did not differ between AZ and KNG (Fig. 3B). The implication was that miR172a is involved in the development of both the spikelet and the rachis. The abundance of miR172b transcript in the spikelet was ~3-fold lower than in the rachis, a ratio that was consistent between AZ and KNG (Fig. 3C).

Localization of mature miR172 and cly1 *transcript*

RNA *in situ* hybridization was conducted on immature spikes at the awn primordium stage to define the sites where mature miR172 and *cly1* transcripts were deposited. Mature miR172 was detected using miRCURY Locked Nucleic Acid (LNA) probes, which deliver enhanced hybridization affinity, sensitivity and specificity. Hybridization with the miR172a probe generated signal in the lodicule primordia and rachis, but not in either the anthers or any other organs (Fig. 4A, E). The pattern of transcript deposition was the same in AZ and KNG (Fig. 4A, E). A similar hybridization profile was obtained when the miR172b probe was used (Fig. 4B, F). When the scrambled miRNA probe was used, no signal was detected (Fig. 4C, G) confirming the specificity of the two miR172 probes. The observed abundance of miR172 in the lodicules was fully consistent with its proposed regulatory role in lodicule development. The *cly1* signal was concentrated in the lodicule

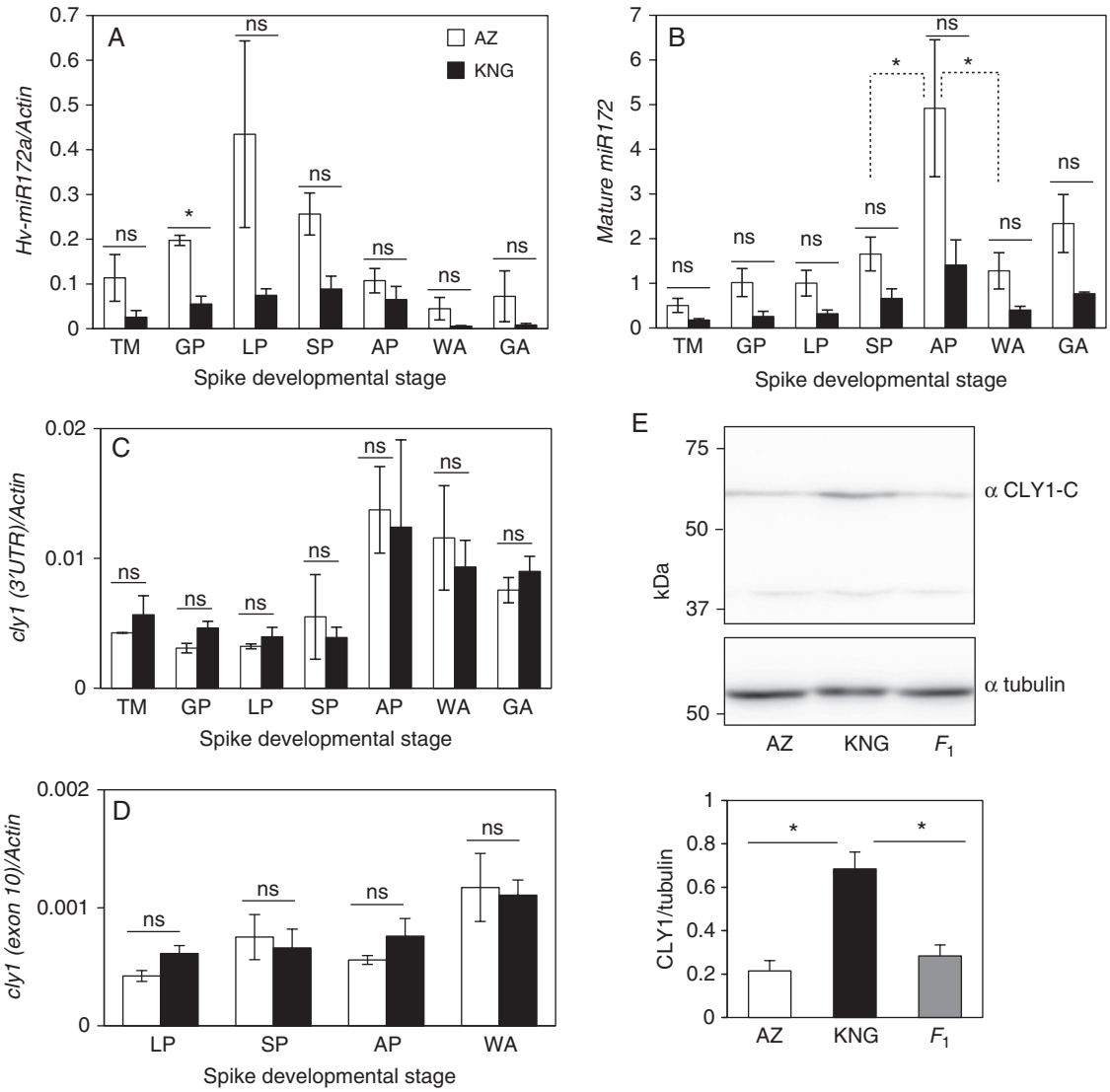

FIG. 2. Expression of miR172 and *cly1*. (A–D) qRT–PCR-derived transcript abundance during spike development of (A) primary miR172a (B) mature miR172 (C) *cly1* (3′-UTR) and (D) *cly1* (exon 10). *Actin* was the chosen reference sequence. TM, triple mound stage; GP, glume primordium stage; LP, lemma primordium stage; SP, stamen primordium stage; AP awn primordium stage; WA, white anther stage; GA, green anther stage. Comparisons between SP and AP and between AP and WA for AZ are shown by the dashed lines in (B). Mean values for KNG were also significantly different between stages at the 5 % probability level. (E) CLY1 western blotting at the white anther stage (top) and abundance as determined by ratio of CLY1/tubulin abundance (bottom). α CLY1-C, anti-CLY1 C-terminal region; α tubulin, anti-tubulin. Values are mean and s.e. (n = 3 biological replications). *Means are significantly different at the 5 % probability level; ns, not significantly different.

primordia in both AZ and KNG (Fig. 4D, H), overlapping the site of miR172 deposition.

Effect of absence of miR172a on lodicule development

The *Ds-miR172a* mutant [#508–72, released as TNP 280, GenBank accession number HM243624 (Brown *et al.*, 2014)] harboured a 3.6-kb *Ds* insertion within the 21-nt miR172 sequence of *Hv-miR172a*, lacked any mature miR172a, and produced an abnormal flower (Brown and Bregitzer, 2011). Since the genetic background of the mutant (cultivar 'Golden Promise') is a *cly1.b* carrier producing small lodicules, it is not possible to infer the effect of the absence of *cly1* regulation by miR172a on lodicule size in the mutant. To examine this, the mutant was crossed and backcrossed with cultivar 'Conlon' (*miR172a/Cly1.a* carriers) to allow the selection of homozygotes in the BC_1F_2 generation for *miR172a/cly1.b*, *miR172a/Cly1.a* and *Ds-miR172a/Cly1.a* (Table 2). The abnormality of flower formation was inherited from the mutant into the derivatives (Fig. 5A). The abnormal spike phenotype of the *Ds* mutant was apparent as early as the glume primordium stage. Inspection of the *Ds-miR172a/Cly1.a* spike revealed branch-like meristems arranged in an indeterminate pattern, in contrast to the single spikelet meristem characteristic of the wild-type spike. In the *Ds* mutant, spikelets containing abnormal and sterile floral structures were formed alongside the normal spikelets (Fig. 5A). The lodicules of *Ds-miR172a/Cly1.a* were very small,

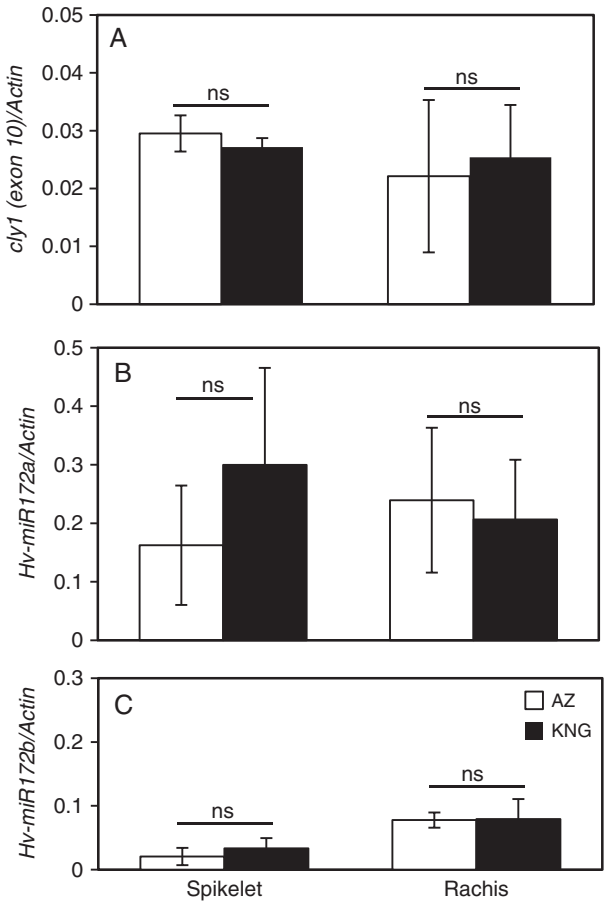

FIG. 3. Abundance of *cly1* and primary miR172 transcripts in the spikelet (flower) and rachis in immature spikes at awn primordium stage. The tissues were laser-microdissected (Supplementary Data Fig. S5). Values are mean and s.e. (n = 3 biological replications). ns, means are not significantly different at the 5 % probability level.

even smaller than those formed by *miR172a/Cly1.a* (Fig. 5B, C). The lodicules formed by the *Ds-miR172a/Cly1.a* genotype were smaller than those formed by *miR172a/cly1.b* (Fig. 5D), which demonstrated the major influence of miR172a on lodicule size (Fig. 5C). Other floral structures were similar with respect to both number and size across all three homozygous genotypes (Fig. 5B–D). The temporal pattern of *cly1* transcription was similar in *miR172a/Cly1.a* homozygotes (WT) and *Ds-miR172a/Cly1.a* homozygotes (*Ds*), and transcript abundances were comparable in the WT and *Ds* (Fig. 5C), a result consistent with transcript abundance in AZ and KNG and translational rather than transcriptional repression. Furthermore, immunoblot analysis showed that the CLY1 level in the *Ds* was higher than that in the WT (Fig. 5F), indicating that the absence of miR172a abolished the suppression of *cly1* translation.

The miR172a *in situ* hybridization signal was detected in the lodicules and rachis of the WT progenitor of the mutant (Fig. 6A) but not in the *Ds-miR172a* mutant (Fig. 6E), confirming that miR172a signal is specific to *Hv-miR172a*. Hybridization with an miR172b probe produced the same profile as generated by miR172a in the WT (Fig. 6B), while in the mutant some low-level signal was present in the rachis but none in the lodicules (Fig. 6F). This result implies that miR172b is not expressed sufficiently to produce signal in lodicules in the absence of miR172a. An alternative explanation could be the possibility of cross-hybridization of miR172b with miR172a in the WT. Signal for *cly1* was detected in both the lodicules and the rachis (Fig. 6D) and the pattern was not disturbed by the absence of miR172a (Fig. 6H).

Expression of barley Q

The *cly1* sequence is related to three other barley HvAP2-like genes, one of which (HvAP2L, GenBank accession number AY069953) is assumed, from phylogenetic analysis (Nair *et al.*, 2010), to be the orthologue of the wheat free-threshing gene Q, Both *Q* and *cly1* encode AP2 proteins of class A of the ABCDE module, which control flower pattering (Luo *et al.*, 2016). The *Q* mRNA sequence has a short sequence complementary to miR172 (Fig. 7A). It was of interest therefore to investigate whether miR172a also interacted with *Q*. An RNA *in situ* hybridization experiment was conducted (Fig. 7B) using as probe a 265-nt 3′-UTR fragment of *Q* (Supplementary Data Fig. S3C, Table S1). The transcript of *Q* was detectable at the triple mound stage in the six-rowed barley cultivar AZ, coinciding with the differentiation of spikelet primordia (Fig. 7B). Transcript was initially restricted to the apex of the triple spikelet meristem, but later spread to the glume primordia and later still to the floral meristem (Fig. 7B). No signal was detected in hybridization with the sense probe for *Q* (negative control) (Fig. 7B).

Both *Ds-miR172a/Cly1.a* and *miR172a/Cly1.a* homozygotes had a similar *Q* localization pattern, where *Q* transcript was concentrated in the spikelet and floral primordia (Fig. 8A). In a comparison of *Q* transcript abundance between *miR172a/Cly1.a* and *Ds-miR172a/Cly1.a*, there was no evidence for any genotypic variation at any of the spike developmental stages sampled (Fig. 8B). This result held whether the amplicon was directed at the 3′-UTR or at exon 10 of *Q* (Supplementary Data Fig. S3C). The spike of the *Ds-miR172a/Cly1.a* genotype exhibited abnormal spikelet development, including the conversion of glumes to florets in the apical regions of the spike and a branching phenotype in the basal region, with each branch consisting of supernumerary spikelets and various floral defects (Fig. 5A). However, the pattern of *Q* transcription did not differ between *Ds-miR172a/Cly1.a* and the WT (Fig. 8B).

DISCUSSION

Identification of mature miR172s and their genes

Although a single nucleotide mismatch at the miR172 binding site within *cly1.b* is sufficient to induce cleistogamy, how *cly1* regulates lodicule development has not been explained as yet. Here, it has been confirmed that mature miR172s are generated in the immature spike, as shown by Nair *et al.* (2010). Studies exploring miRNAs in barley through a computational approach (Colaiacovo *et al.*, 2010) or by means of next-generation sequencing technology (Schreiber *et al.*, 2011; Curaba *et al.*, 2012; Lv *et al.*, 2012; Ozhuner *et al.*, 2013; Hackenberg

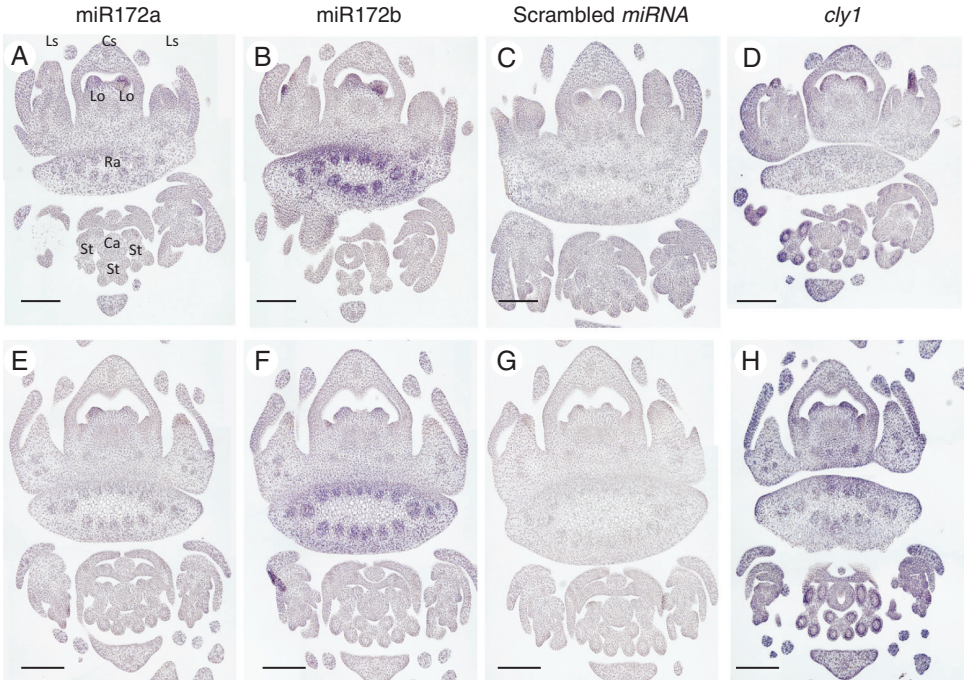

FIG. 4. Localization of mature miR172s and *cly1* by RNA *in situ* hybridization in the immature spike sampled at the awn primordium stage. Plant genotypes were AZ (*Cly1.a*) (A–D) and KNG (*cly1.b*) (E–H). Spike RNAs were hybridized with miR172a probe (A, E), miR172b probe (B, F), scrambled miRNA probe (negative control) (C, G) and *cly1* probe (D, H). Cs, central spikelet; Ls, lateral spikelet; Lo, lodicule; Ra, rachis; Ca, carpel; St, stamen. Scale bars = 0.1 mm.

TABLE 2. *Spike phenotypes in plants with different combinations of* Hv-miR172a *and* cly1 *alleles*

Crosses	Line	Locus		Lodicules			Determinacy[a]
		Hv-miR172a	*cly1*	Width (mm) mean ± s.e.	Depth (mm) mean ± s.e.	Overall size	
Parents	'Conlon'	*miR172a*	*Cly1.a*	1.14 ± 0.12	1.12 ± 0.16	Large	Wild-type
	'Morex'	*miR172a*	*Cly1.a*	0.94 ± 0.08	1.11 ± 0.18	Large	Wild-type
	GP	*miR172a*	*cly1.b*	0.46 ± 0.05	0.28 ± 0.04	Small	Wild-type
	#508-72[b]	*Ds-miR172a*	*cly1.b*	0.19 ± 0.01	0.19 ± 0.01	Rudimentary	Indeterminate
Conlon*2/#508-72[c]	TC11-7 #5	*miR172a*	*Cly1.a*	0.86 ± 0.09	1.00 ± 0.04	Large	Wild-type
	TC11-7 #4	*miR172a*	*cly1.b*	0.35 ± 0.03	0.41 ± 0.01	Small	Wild-type
	TC11-7 #1	*Ds-miR172a*	*Cly1.a*	0.22 ± 0.05	0.21 ± 0.02	Rudimentary	Indeterminate
Morex*2/#508-72[c]	TC11-9 #1	*miR172a*	*Cly1.a*	0.82 ± 0.07	0.81 ± 0.04	Large	Wild-type
	TC11-9 #4	*miR172a*	*cly1.b*	0.42 ± 0.07	0.40 ± 0.06	Small	Wild-type
	TC11-9 #14	*Ds-miR172a*	*Cly1.a*	0.19 ± 0.03	0.16 ± 0.04	Rudimentary	Indeterminate

[a]Spike and spikelet meristem determinacy.
[b]*Ds-miR172a* mutant in GP.
[c]BC_1F_2 generation; lines were homozygous for the mentioned loci.

et al., 2015) reported the presence of miR172s in barley tissues, but none of these studies validated the precursor structure and described an miR172 gene. We have shown experimental evidence for barley miR172s, their precursors and primary transcripts, as well as their gene function. An effort was made here to quantify the abundance of miR172 sequences, using both qRT–PCR and sRNA sequencing. The clear result was that the predominant isoform of the three identified was miR172a. Analysis of various species has shown that miR172 is encoded by multiple loci (five in both *Arabidopsis thaliana* and maize, four in rice), although in some cases more than one gene has been shown to encode an identical mature isoform (Zhu and Helliwell, 2011). A survey of the barley genome sequence indicated that barley harbours three miR172 genes, although the current incomplete state of the genome sequence means that the final number may be greater than this. The predicted miR172 precursor structures were as expected, insofar as the mature sequences were all located on the 3′ arm of the transcript (Bartel and Bartel, 2003; Jones-Rhoades, 2012). The length and folding free energy of the precursors also lay within the expected range, and sequence conservation only applied to the mature miR172 and its complementary sequences, as is the general case for

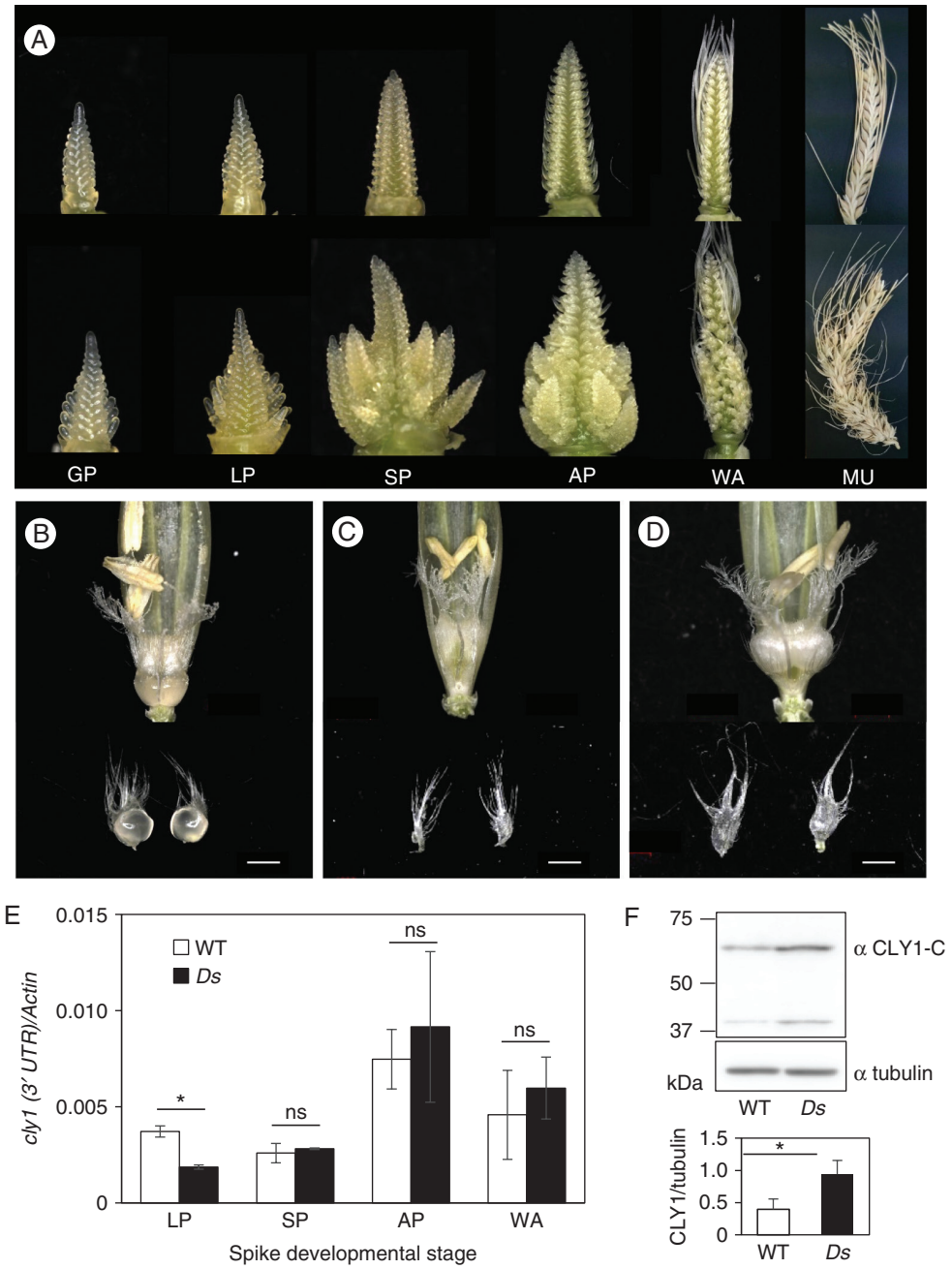

FIG. 5. Effect of absence of miR172a on inflorescence phenotype and accumulation of CLY1. (A) *miR172a/Cly1.a* (top) and *Ds-miR172a/Cly1.a* (bottom) at stages from glume primordium (GP) to maturity (MU). LP, lemma primordium stage; SP, stamen primordium stage; AP, awn primordium stage; WA, white anther stage. (B–D) Variation in lodicule size at anthesis in (B) *miR172a/Cly1.a* homozygote (C) *Ds-miR172a/Cly1.a* homozygote and (D) *miR172a/cly1.b* homozygote. Scale bars = 1 mm. (E) qRT–PCR-derived transcript abundance of *cly1*. *Actin* was the reference transcript. (F) Western blot analysis of CLY1 in *miR172a/Cly1.a* (WT) and *Ds-miR172a/Cly1.a* (*Ds*) (top) and abundance as determined by ratio of CLY1/tubulin abundance (bottom). Values in (E) and (F) are mean and s.e. ($n = 3$ biological replications). *Means are significantly different at the 5 % probability level; ns, not significantly different.

miRNAs (Bartel, 2004; Jones-Rhoades, 2012). The indications are therefore that the three barley miR172 loci *Hv-miR172a* (encoding *miRNA172a*), *Hv-miR172b* (encoding *miRNA172b*) and *Hv-miR172c* (encoding *miRNA172c*) are all authentic.

The abundance of mature plant miRNAs generated from their various genes is known to vary across growth stages and/or tissue types (Zhu and Helliwell, 2011). All three barley miR172 genes were transcribed in the immature spike, although miR172a was the dominant isoform, thereby implicating it as the leading candidate as the *cly1* regulator. It was not possible to exclude the participation of miR172b because of its presence in both the lodicule and rachis, and no miR172b knockout mutant has as yet been isolated. The abundance of pri-miR172a was particularly high at the early stages of spike development, but the abundance of the mature form peaked rather later. Examples are known where pri-miRNAs are detectable but

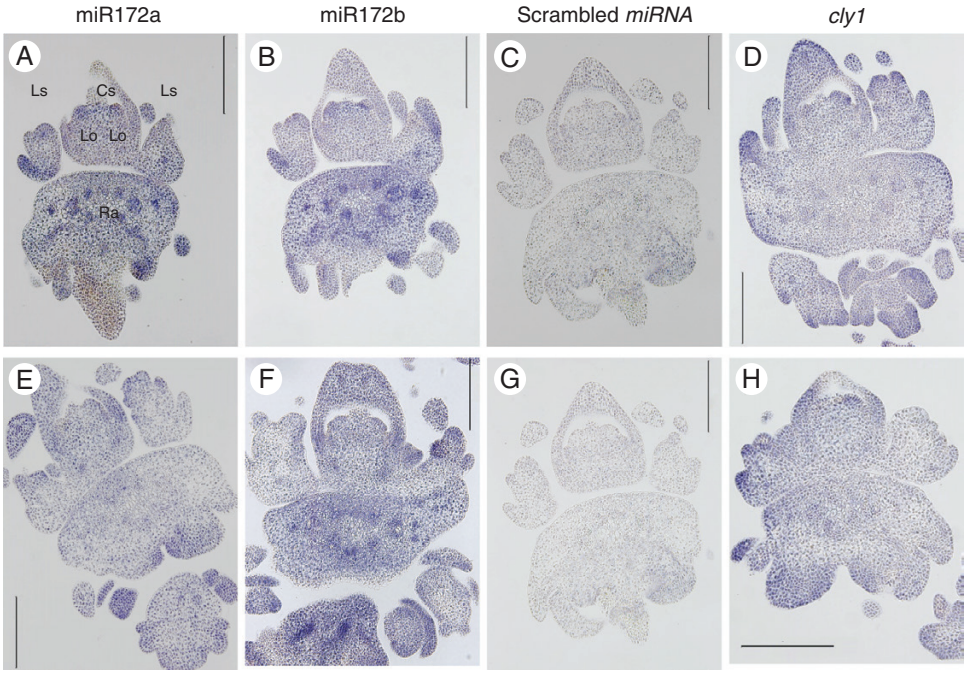

FIG. 6. Effect of absence of miR172a on accumulation of miR172 and *cly1* transcripts in the immature spike sampled at the awn primordium stage. Plant genotypes were *miR172a/Cly1.a* (A–D) and *Ds-miR172a/Cly1.a* (E–H). Spike RNAs were hybridized with miR172a (A, E), miR172b (B, F), scrambled miRNA (negative control) (C, G) and *cly1* (D, H). Cs, central spikelet; Ls, lateral spikelet; Lo, lodicule; Ra, rachis. Scale bars = 0.2 mm.

their mature products are not, or at least are only present at a lesser abundance (Ambros *et al.*, 2003; Michael *et al.*, 2003; Wulczyn *et al.*, 2007; Lee *et al.*, 2008). The implication was that pri-miR172s remained unprocessed until required (Jung *et al.*, 2007). The abundance of both pri-miR172a and mature miR172s was particularly high in AZ, suggesting a transcriptional difference between AZ and KNG. This is consistent with the known role of AP2 in repressing miR172 transcription (Yant *et al.*, 2010). Thus, in addition to differences in miR172 and target association due to sequence complementarity, which influences translation between the cultivars, having more of the miR172 may also act as a feedback loop to keep CLY1 levels down.

miR172a is essential for the development of the lodicule

The abundance of miR172 isoforms varies both spatially and temporally, contributing to their functional divergence (Yumul *et al.*, 2013). When miR172a is absent, as in the *Ds*-induced *Hv-miR172a* knockout mutant (Brown and Bregitzer, 2011), the lodicule fails to develop normally, resulting in cleistogamous flowering. Thus miR172a activity is clearly required for non-cleistogamy. In rice, the overexpression of *Os-miR172b* (which generates a mature product identical to miR172a) induces larger (or a greater number of) lodicules (Zhu *et al.*, 2009), suggesting that the barley and rice orthologues have an equivalent function. Overexpressors of *Os-miR172a* (which generates a mature product identical to miR172b) exhibit no distinct phenotype (Zhu *et al.*, 2009), while the *A. thaliana* double loss-of-function mutant miR172a/miR172b (both genes generate a mature product identical to miR172b) similarly produces a WT flower (Zhao *et al.*, 2007). Laser microdissection was used in the present study in an attempt to quantify miR172a and miR172b in a more precisely defined site, the spikelets separated from the rachis. What emerged was that miR172a was more abundant than miR172b. As the barley miR172a and miR172b sequences differed by a just a single nucleotide, this polymorphism might be responsible for their distinct biological functions.

miR172a downregulates the translation of CLY1

The increasing abundance of both mature miR172a and *cly1* transcript as spike development proceeded is consistent with their biological interaction during lodicule growth. Not only was the accumulation of the transcripts quantified here, but also their site of deposition. The localization of miR172a within the lodicules supports the hypothesis that it is a determinant of lodicule development; at the same time, *cly1* message accumulated in the lodicules, as also reported by Nair *et al.* (2010). In the lodicules of AZ, both miR172a and *cly1* transcript accumulated, demonstrating that the presence of miR172a in itself did not deplete *cly1* transcript. The abundance of *cly1* transcript in AZ and KNG was almost identical, and the RNA *in situ* analysis showed that *cly1* transcript was concentrated within both the lodicules and the anthers. The inference is that the AZ and KNG lodicules harbour a similar abundance of *cly1* transcript. The implication was that miR172 regulated the translation of the *cly1*. This hypothesis was therefore tested by immunoblotting.

miR172s have been reported to regulate not only the abundance of *AP2* transcript through transcript cleavage, but also to inhibit *AP2* translation (Aukerman and Sakai, 2003; Kasschau

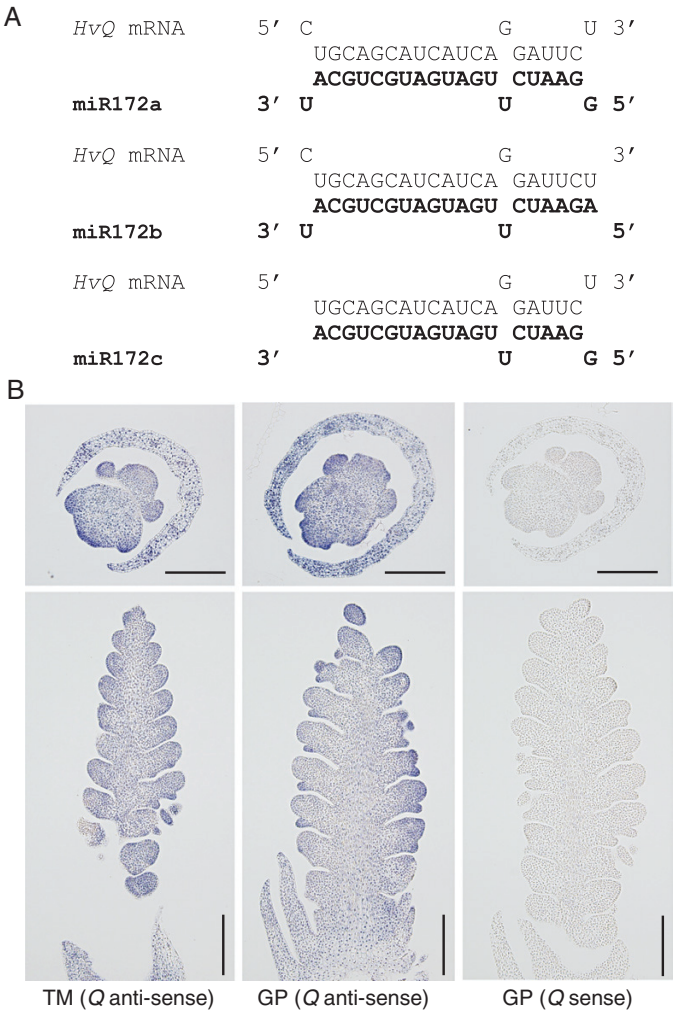

FIG. 7. Interaction of barley *Q* with miR172. (A) Potential interactions between *Q* mRNA and miR172 isoforms ('Morex'). (B) Localization of *Q* mRNA in the immature spike sampled at the triple mound (TM) and glume primordium (GP) stages in AZ, as detected by RNA *in situ* hybridization with an anti-sense and sense *Q* (3′-UTR) transcript. Scale bars = 0.2 mm in horizontal sections and 1 mm in longitudinal sections of immature spikes.

et al., 2003; Chen, 2004; Schwab *et al.*, 2005; Jung *et al.*, 2007; Zhu *et al.*, 2009). It was not practically feasible to recover sufficient RNA from the lodicule primordia, but *cly1* transcript abundance was successfully measured separately in the spikelets and the rachis. Lodicules are the only organs where *cly1* and miR172 expression overlaps within a spikelet. The abundance of *cly1* transcript in laser-microdissected spikelet sections is likely to represent the *cly1* transcript abundance in lodicules. The lack of any difference in *cly1* transcript abundance in these two floral parts, both in AZ and KNG, lent strong support to the proposition that *cly1* transcript is not degraded in non-cleistogamous cultivars. A similar conclusion has been drawn in both *A. thaliana* and rice (Jung *et al.*, 2007; Zhu *et al.*, 2009). Comparable *cly1* transcript abundances were obtained in AZ and KNG, irrespective of whether the primers flanked the miR172 target site or were directed to the *cly1* 3′-UTR. Nair *et al.* (2010) suggested that miR172 directed transcript suppression of *cly1* based on the detection of *cly1* cleaved products by 5′-RACE (rapid amplification of cDNA ends) PCR in non-cleistogamous barley. qRT–PCR reported by Nair *et al.* (2010) and the present study showed no significant difference in *cly1* transcript accumulation between AZ and KNG. *In situ* hybridization also clearly detected signal in lodicules of both the non-cleistogamous and cleistogamous types. These results imply that *cly1* transcripts cleaved by miR172 represent only a small proportion of the entire set of *cly1* transcripts, and they do not act to regulate the control exerted by CLY1 over lodicule development. In *A. thaliana*, even though cleavage products of the *cly1* orthologue *AtAP2* were detectable using 5′-RACE PCR, it was undetectable using northern blot analysis, a method free from PCR-oriented bias (Aukerman and Sakai, 2003). The suggestion was therefore that miR172-directed cleavage products of *AP2* transcripts are rare and their presence is not indicative of miR172 function (Aukerman and Sakai, 2003; Chen, 2004).

The alternative mechanism by which miR172a controls *cly1* regulation is by the repression of *cly1* translation. Many studies during the past 15 years have established translational repression as a prominent mode of action by miR172 rather than mRNA cleavage in plants (Zhu and Helliwell, 2011; Ma *et al.*, 2013). If miR172a influences *cly1* translation, then the expectation is that less CLY1 protein would be accumulated in non-cleistogamous cultivars. The immunoblot analysis indeed revealed a reduced accumulation of CLY1 in the AZ spike compared with the level in the KNG spike. The ability of miR172a to interfere with *cly1* translation was further confirmed by the behaviour of the *Ds*-induced loss of function of the *Hv-miR172a* mutant, which exhibited an increased accumulation of CLY1. The increased accumulation of CLY1 always resulted in reduced (KNG) or rudimentary (*Ds-miR172a*) lodicule size, in accordance with the notion that CLY1 protein is the suppressor of lodicule development (Nair *et al.*, 2010).

Perspective of miR172-directed spike determinacy

The spikelet indeterminacy and overall floral defects exhibited by the *Ds-miR172a* mutant were comparable with the phenotype of the *SNB* loss-of-function mutant in rice (Lee *et al.*, 2006). The abnormal spike phenotype of the miR172a knockout mutant was also reminiscent of that produced by the maize *miR172* mutant (*ts4*), in which *IDS1* (the *Q* orthologue) is no longer regulated (Chuck *et al.*, 2007). The glume-to-floret transition in apical spikelets of the *Ds-miR172a* mutant was similar to that observed in wheat with higher *Q* activity (Greenwood *et al.*, 2017) or lower miR172 activity (Debernardi *et al.*, 2017). The miR172-directed regulation of *AP2*-like genes is important for floral transition and floral patterning in cereals (Zhu and Helliwell, 2011; Luo *et al.*, 2013). *miR172-AP2*-like *(SNB/OsIDS1)* modules control the conversion of the spikelet meristem into the floral meristem in rice and maize (Luo *et al.*, 2013). The *AP2-like* orthologous gene *Q* has been well characterized in wheat (Simons *et al.*, 2006) and has recently been shown to be regulated by miR172 in relation to spike morphology and the freethreshing character (Debernardi *et al.*, 2017;

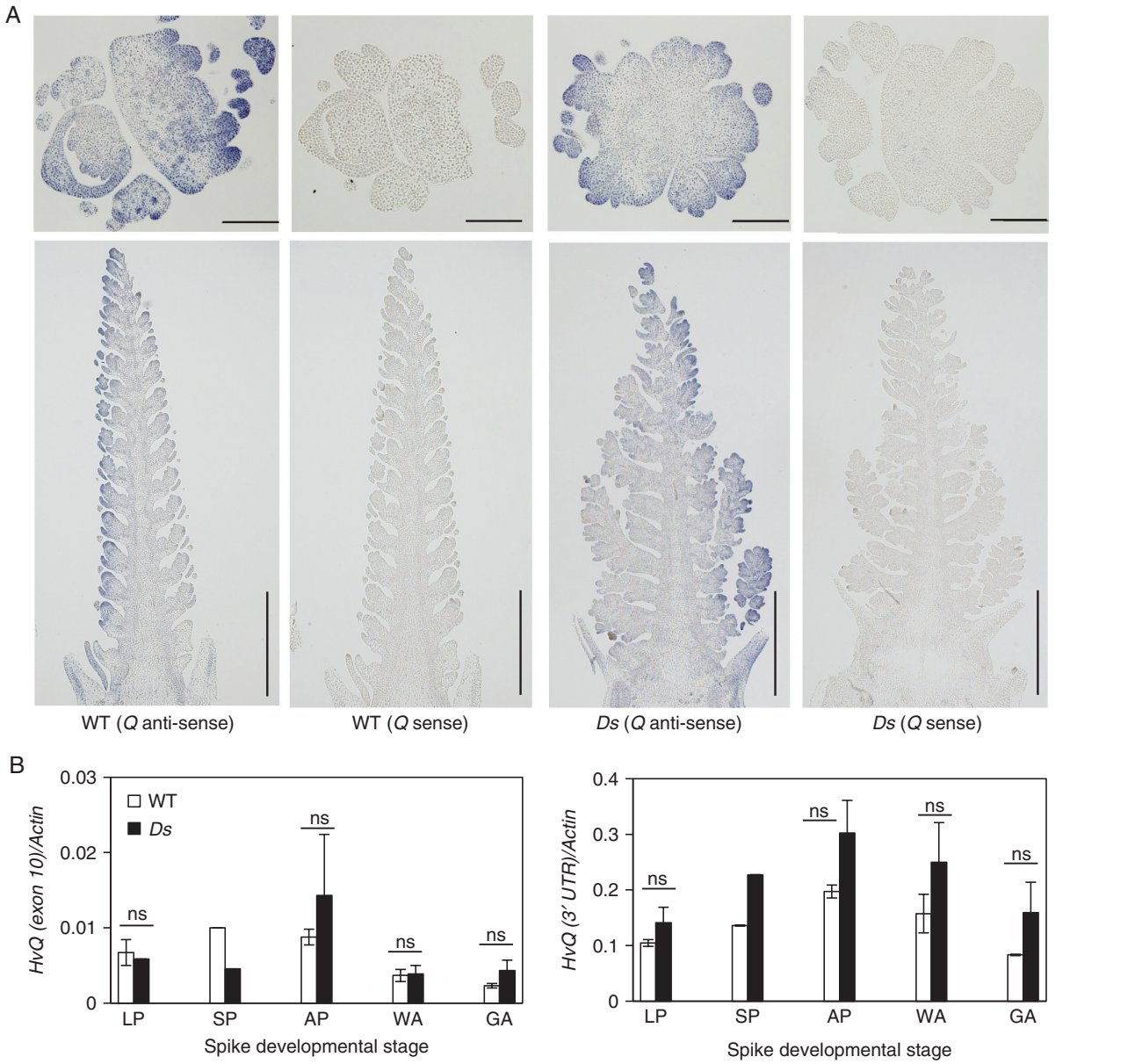

FIG. 8. Expression of *Q* in immature barley spikes. (A) Localization of *Q* mRNA in an immature spike sampled at the awn primordium stage of WT (*miR172a/Cly1*) and *Ds* (*Ds-miR172a/Cly1*), as detected by *in situ* hybridization with an anti-sense and sense *Q* (3′-UTR) transcript. Scale bars = 0.2 mm in horizontal sections and 1 mm in longitudinal sections. (B) qRT–PCR-derived transcript abundance of *Q* during spike development in WT (*miR172a/Cly1*) and *Ds* (*Ds-miR172a/Cly1*). Values are mean and s.e. ($n = 3$ biological replications). LP, lemma primordium stage; SP, stamen primordium stage; AP, awn primordium stage; WA, white anther stage; GA, green anther stage. ns, means are not significantly different at the 5 % probability level.

Greenwood *et al.*, 2017; Liu *et al.*, 2017). However, the barley *Q* gene and the possible role of miR172 in its regulation in the determination of spike morphology. It was clear from the present experiments that miR172 does not compromise the abundance of barley *Q* transcript, agreeing with the cases of both *IDS1* (Chuck *et al.*, 2007) and *SNB* (Zhu *et al.*, 2009). The present data suggest that miR172 may influence meristem fate in the barley inflorescence presumably by targeting *AP2*-like genes; *Q* may be one of the candidate genes, but interaction between miR172 and *AP2*-like genes for barley spike determinacy requires additional evidence.

SUPPLEMENTARY DATA

Supplementary data are available online at https://academic.oup.com/aob and consist of the following. Table S1: list of primers and probes. Figure S1: detection of barley miRNAs capable of interaction with *cly1* in cultivar 'Morex' immature spikes. Figure S2: alignment of *Hv-miR172* precursors with the top hits from miR172 precursors in miRBase. Figure S3: positions of primers and probes used for gene expression analysis. Figure S4: PCR amplification efficiency of qRT–PCR primers. Figure S5: flower and rachis tissues isolated from immature spikes at the awn primordium stage by laser microdissection.

ACKNOWLEDGEMENTS

We thank Ning Wang for help in antibody design, Shun Sakuma for help in qRT–PCR, Nils Stein for access to the barley genome sequences, Harumi Koyama for taking care of the plants and helping to sample the spikes, Hisae Kamakura for preparing material for laser microdissection, and the NIAS Genebank (Tsukuba, Japan) for the provision of seeds of the various barley cultivars. This research was supported by the Japanese Ministry of Agriculture, Forestry and Fisheries Genomics for Agricultural Innovation programme (TRS1001 to J.W. and TRS1002 and TRS1005 to T.K.).

LITERATURE CITED

Abdel-Ghani AH, **Parzies HK**, **Omary A**, **Geiger HH. 2004**. Estimating the outcrossing rate of barley landraces and wild barley populations collected from ecologically different regions of Jordan. *Theoretical and Applied Genetics* **109**: 588–595.

Ambros V, **Lee RC**, **Lavanway A**, **Williams PT**, **Jewell D. 2003**. MicroRNAs and other tiny endogenous RNAs in *C. elegans*. *Current Biology* **13**: 807–818.

Aukerman MJ, **Sakai H. 2003**. Regulation of flowering time and floral organ identity by a microRNA and its *APETALA2*-like target genes. *Plant Cell* **15**: 2730–2741.

Bartel B, **Bartel DP. 2003**. MicroRNAs: at the root of plant development. *Plant Physiology* **132**: 709–717.

Bartel DP. 2004. MicroRNAs: genomics, biogenesis, mechanism, and function. *Cell* **116**: 281–297

Bommert P, **Satoh-Nagasawa N**, **Jackson D**, **Hirano HY. 2005**. Genetics and evolution of inflorescence and flower development in grasses. *Plant and Cell Physiology* **46**: 69–78.

Briggs D. 1978. *Barley*. London: Chapman and Hall.

Brown R, **Dahleen LS**, **Lemaux PG**, **Bregitzer P. 2014**. Registration of the barley transposon-tagged population I: seventy lines each with a single, unique site of *Ds* insertion. *Journal of Plant Registration* **8**: 226–230.

Brown RH, **Bregitzer P. 2011**. A *Ds* insertional mutant of a barley miR172 gene results in indeterminate spikelet development. *Crop Science* **51**: 1664–1672.

Camacho C, **Coulouris G**, **Avagyan V**, ***et al.* 2009**. BLAST+: architecture and applications. *BMC Bioinformatics* **10**: 421.

Chen X. 2004. A microRNA as a translational repressor of *APET ALA2* in *Arabidopsis* flower development. *Science* **303**: 2022–2025.

Chuck G, **Meeley R**, **Irish E**, **Sakai H**, **Hake S. 2007**. The maize *tasselseed4* microRNA controls sex determination and meristem cell fate by targeting *Tasselseed6/indeterminate spikelet1*. *Nature Genetics* **39**: 1517–1521.

Ciaffi M, **Paolacci AR**, **Tanzarella OA**, **Porceddu E. 2011**. Molecular aspects of flower development in grasses. *Sexual Plant Reproduction* **24**: 247–282.

Colaiacovo M, **Subacchi A**, **Bagnaresi P**, **Lamontanara A**, **Cattivelli L**, **Faccioli P. 2010**. A computational-based update on microRNAs and their targets in barley (*Hordeum vulgare* L.). *BMC Genomics* **11**: 595.

Curaba J, **Spriggs A**, **Taylor J**, **Li Z**, **Helliwell C. 2012**. miRNA regulation in the early development of barley seed. *BMC Plant Biology* **12**: 120.

Dai X, **Zhao PX. 2011**. psRNATarget: a plant small RNA target analysis server. *Nucleic Acids Research* **39**: W155–W159.

Daniell H. 2002. Molecular strategies for gene containment in transgenic crops. *Nature Biotechnology* **20**: 581–586.

Debernardi JM, **Lin H**, **Chuck G**, **Faris JD**, **Dubcovsky J. 2017**. microRNA172 plays a crucial role in wheat spike morphogenesis and grain threshability. *Development* **144**: 1966–1975.

Gines M, **Baldwin T**, **Rashid A**, ***et al.* 2017**. Selection of expression reference genes with demonstrated stability in barley among a diverse set of tissues and cultivars. *Crop Science* **58**: 332–341.

Greenwood J, **Finnegan JE**, **Watanabe N**, **Trevaskis B**, **Swain SM. 2017**. New alleles of the wheat domestication gene *Q* reveal multiple roles in growth and reproductive development. *Development* **144**: 1959–1965.

Hackenberg M, **Gustafson P**, **Langridge P**, **Shi BJ. 2015**. Boron stress responsive microRNAs and their targets in differential expression of microRNAs and other small RNAs in barley between water and drought conditions. *Plant Biotechnology Journal* **13**: 2–13.

Honda I, **Turuspekov Y**, **Komatsuda T**, **Watanabe Y. 2005**. Morphological and physiological analysis of cleistogamy in barley (*Hordeum vulgare*). *Physiologia Plantarum* **124**: 524–531.

Hori K, **Sato K**, **Kobayashi T**, **Takeda K. 2006**. QTL analysis of fusarium head blight severity in recombinant inbred population derived from a cross between two-rowed barley varieties. *Breeding Science* **56**: 25–30.

Jones-Rhoades MW. 2010. Prediction of plant miRNA genes. *Methods in Molecular Biology* **592**: 19–30.

Jones-Rhoades MW. 2012. Conservation and divergence in plant microRNAs. *Plant Molecular Biology* **80**: 3–16.

Jones-Rhoades MW, **Bartel DP. 2004**. Computational identification of plant microRNAs and their targets, including a stress-induced miRNA. *Molecular Cell* **14**: 787–799.

Joshi T, **Yan Z**, **Libault M**, ***et al.* 2010**. Prediction of new miRNAs and associated target genes in *Glycine max*. *BMC Bioinformatics* **11**: S14-10.1186/1471-2105-11-S1-S14.

Jung JH, **Seo YH**, **Seo PJ**, ***et al.* 2007**. The *GIGANTEA*-regulated microRNA172 mediates photoperiodic flowering independent of *CONSTANS* in *Arabidopsis*. *Plant Cell* **19**: 2736–2748.

Kasschau KD, **Xie Z**, **Allen E**, ***et al.* 2003**. P1/HC-Pro, a viral suppressor of RNA silencing, interferes with *Arabidopsis* development and miRNA function. *Developmental Cell* **4**: 205–217.

Kim B, **Yu HJ**, **Park SG**, ***et al.* 2012**. Identification and profiling of novel microRNAs in the *Brassica rapa* genome based on small RNA deep sequencing. *BMC Plant Biology* **12**: 218.

Kirby EJM, **Appleyard M. 1981**. *Cereal development guide*. Kenilworth: NAC Cereal Unit.

Komatsuda T, **Nakamura I**, **Takaiwa F**, **Oka S. 1998**. Development of STS markers closely linked to the *vrs1* locus in barley, *Hordeum vulgare*. *Genome* **41**: 680–685.

Komatsuda T, **Pourkheirandish M**, **He C**, ***et al.* 2007**. Six-rowed barley originated from a mutation in a homeodomain-leucine zipper I-class homeobox gene. *Proceedings of the National Academy of Sciences of the USA* **104**: 1424–1429.

Korhonen J, **Martinmäki P**, **Pizzi C**, **Rastas P**, **Ukkonen E. 2009**. MOODS: fast search for position weight matrix matches in DNA sequences. *Bioinformatics* **25**: 3181–3182.

Kozomara A, **Griffiths-Jones S. 2011**. miRBase: integrating microRNA annotation and deep-sequencing data. *Nucleic Acids Research* **39**: D152–D157.

Langmead B, **Trapnell C**, **Pop M**, **Salzberg SL. 2009**. Ultrafast and memory-efficient alignment of short DNA sequences to the human genome. *Genome Biology* **10**: R25.

Lauter N, **Kampani A**, **Carlson S**, **Goebel M**, **Moose SP. 2005**. *microRNA172* down-regulates *glossy15* to promote vegetative phase change in maize. *Proceedings of the National Academy of Sciences of the USA* **102**: 9412–9417.

Lee DY, **Lee J**, **Moon S**, **Park SY**, **An G. 2006**. The rice heterochronic gene *SUPERNUMERARY BRACT* regulates the transition from spikelet meristem to floral meristem. *Plant Journal* **49**: 64–78.

Lee EJ, **Baek M**, **Gusev Y**, **Brackett DJ**, **Nuovo GJ**, **Schmittgen TD. 2008**. Systematic evaluation of microRNA processing patterns in tissues, cell lines, and tumors. *RNA* **14**: 35–42.

Lelandais-Briere C, **Naya L**, **Sallet E**, ***et al.* 2009**. Genome-wide *Medicago truncatula* small RNA analysis revealed novel microRNAs and isoforms differentially regulated in roots and nodules. *Plant Cell* **21**: 2780–96.

Liu P, **Liu J**, **Dong H**, **Sun J. 2017**. Functional regulation of *Q* by microRNA172 and transcriptional co-repressor TOPLESS in controlling bread wheat spikelet density. *Plant Biotechnology Journal* **16**: 495–506.

Livak KJ, **Schmittgen TD. 2001**. Analysis of relative gene expression data using real-time quantitative PCR and the $2^{-2DC}{}_{T}$ method. *Methods* **25**: 402–408.

Lord EM. 1981. Cleistogamy – a tool for the study of floral morphogenesis, function and evolution. *Botanical Review* **47**: 421–449.

Luo Y, **Guo Z**, **Li L. 2013**. Evolutionary conservation of microRNA regulatory programs in plant flower development. *Developmental Biology* **380**: 133–144.

Luo Y, **Hu JY**, **Li L**, **Luo YL**, **Wang PF**, **Song BH. 2016**. Genome-wide analysis of gene expression reveals gene regulatory networks that regulate

chasmogamous and cleistogamous flowering in *Pseudostellaria heterophylla* (Caryophyllaceae). *BMC Genomics* **17**: 382.

Lv S, **Nie X**, **Wang L**, **Du X**, **Biradar SS**, **Jia X**, **Weining S. 2012**. Identification and characterization of microRNAs from barley (*Hordeum vulgare* L.) by high-throughput sequencing. *International Journal of Molecular Sciences* **13**: 2973–2984.

Ma SM, **Wang YF. 2004**. Molecular strategies for decreasing the gene flow of transgenic plants. *Yi Chuan* **26**: 556–559.

Ma X, **Cao X**, **Mo B**, **Chen X. 2013**. Trip to ER: microRNA-mediated translational repression in plants. *RNA Biology* **10**: 1586–1592.

Mateos JL, **Bologna NG**, **Chorostecki U**, **Palatnik JF. 2010**. Identification of microRNA processing determinants by random mutagenesis of *Arabidopsis* MIR172a precursor. *Current Biology* **20**: 49–54.

Mayer KFX, **Waugh R**, **Langridge P**, ***et al.* 2012**. A physical, genetic and functional sequence assembly of the barley genome. *Nature* **491**: 711–716.

Michael MZ, **van Holst SMOC**, **Pellekaan NG**, **Young GP**, **James RJ. 2003**. Reduced accumulation of specific microRNAs in colorectal neoplasia. *Molecular Cancer Research* **1**: 882–891.

Nair SK, **Wang N**, **Turuspekov Y**, ***et al.* 2010**. Cleistogamous flowering in barley arises from the suppression of microRNA-guided *HvAP2* mRNA cleavage. *Proceedings of the National Academy of Sciences of the USA* **107**: 490–495.

Ozhuner E, **Eldem V**, **Ipek A**, ***et al.* 2013**. Boron stress responsive microRNAs and their targets in barley. *PLoS ONE* **8**: e59543.

Park W, **Li J**, **Song R**, **Messing J**, **Chen X. 2002**. CARPEL FACTORY, a Dicer homolog, and HEN1, a novel protein, act in microRNA metabolism in *Arabidopsis thaliana*. *Current Biology* **12**: 1484–1495.

Qiu CX, **Xie FL**, **Zhu YY**, ***et al.* 2007**. Computational identification of microRNAs and their targets in *Gossypium hirsutum* expressed sequence tags. *Gene* **395**: 49–61.

Sato K, **Hori K**, **Takeda K. 2008**. Detection of fusarium head blight resistance QTLs using five populations of top-cross progeny derived from two-row × two-row crosses in barley. *Molecular Breeding* **22**: 517–526.

Schmid M, **Uhlenhaut NH**, **Godard F**, ***et al.* 2003**. Dissection of floral induction pathways using global expression analysis. *Development* **130**: 6001–6012.

Schreiber AW, **Shi BJ**, **Huang CY**, **Langridge P**, **Baumann U. 2011**. Discovery of barley miRNAs through deep sequencing of short reads. *BMC Genomics* **12**: 129.

Schwab R, **Palatnik JF**, **Riester M**, **Schommer C**, **Schmid M**, **Weigel D. 2005**. Specific effects of microRNAs on the plant transcriptome. *Developmental Cell* **8**: 517–527.

Simons KJ, **Fellers JP**, **Trick HN**, ***et al.* 2006**. Molecular characterization of the major wheat domestication gene *Q*. *Genetics* **172**: 547–555.

Stojanova B, **Maurice S**, **Cheptou PO. 2016**. Is plasticity across seasons adaptive in the annual cleistogamous plant *Lamium amplexicaule*? *Annals of Botany* **117**: 681–691.

Takahashi H, **Kamakura H**, **Sato Y**, ***et al.* 2010**. A method for obtaining high quality RNA from paraffin sections of plant tissues by laser microdissection. *Journal of Plant Research* **123**: 807–813.

Turuspekov Y, **Mano Y**, **Honda I**, **Kawada N**, **Watanabe Y**, **Komatsuda T. 2004**. Identification and mapping of cleistogamy genes in barley. *Theoretical and Applied Genetics* **109**: 480–487.

Wang N, **Ning S**, **Wu J**, **Tagiri A**, **Komatsuda T. 2015**. An epiallele at *cly1* affects the expression of floret closing (cleistogamy) in barley. *Genetics* **199**: 95–104.

Wulczyn FG, **Smirnova L**, **Rybak A**, ***et al.* 2007**. Post-transcriptional regulation of the *let-7* microRNA during neural cell specification. *FASEB Journal* **21**: 415–426.

Xie FL, **Huang SQ**, **Guo K**, ***et al.* 2007**. Computational identification of novel microRNAs and targets in *Brassica napus*. *FEBS Letters* **581**: 1464–1474.

Xie Z, **Allen E**, **Fahlgren N**, **Calamar A**, **Givan SA**, **Carrington JC. 2005**. Expression of *Arabidopsis MIRNA* genes. *Plant Physiology* **138**: 2145–2154.

Yant L, **Mathieu J**, **Dinh T**, ***et al.* 2010**. Orchestration of the floral transition and floral development in *Arabidopsis* by the bifunctional transcription factor APETALA2. *Plant Cell* **22**: 2156–2170.

Yoshida M, **Kawada N**, **Tahnooka T. 2005**. Effect of row type, flowering type and several other spike characters on resistance to fusarium head blight in barley. *Euphytica* **141**: 217–227.

Yumul RE, **Kim YJ**, **Liu X**, ***et al.* 2013**. *POWERDRESS* and diversified expression of the MIR172 gene family bolster the floral stem cell network. *PLoS Genetics* **9**: e1003218.

Zhang BH, **Pan XP**, **Cox B**, **Coob GP**, **Anderson TA. 2006**. Evidence that miRNAs are different from other RNAs. *Cellular and Molecular Life Sciences* **63**: 246–254.

Zhao L, **Kim Y**, **Dinh TT**, **Chen X. 2007**. miR172 regulates stem cell fate and defines the inner boundary of *APETALA3* and *PISTILLATA* expression domain in *Arabidopsis* floral meristems. *Plant Journal* **51**: 840–849.

Zhu Q, **Helliwell CA. 2011**. Regulation of flowering time and floral patterning by miR172. *Journal of Experimental Botany* **62**: 487–495.

Zhu QH, **Upadhyaya NM**, **Gubler F**, **Helliwell CA. 2009**. Overexpression of miR172 causes loss of spikelet determinacy and floral organ abnormalities in rice (*Oryza sativa*). *BMC Plant Biology* **9**: 149.

Zuker M. 2003. Mfold web server for nucleic acid folding and hybridization prediction. *Nucleic Acids Research* **31**: 3406–3415.